Role of the ρ meson in the description of pion electroproduction experiments

Amand Faessler,[1] Thomas Gutsche,[1] Valery E. Lyubovitskij,[1,*] and Igor T. Obukhovsky[2]

[1]*Institut für Theoretische Physik, Universität Tübingen, Auf der Morgenstelle 14, D-72076 Tübingen, Germany*
[2]*Institute of Nuclear Physics, Moscow State University, RU-119899 Moscow, Russia*

We study the $p(e, e'\pi^+)n$ reaction in the framework of an effective Lagrangian approach including nucleon, π and ρ meson degrees of freedom and show the importance of the ρ-meson t-pole contribution to σ_T, the transverse part of cross section. We test two different field representations of the ρ meson, vector and tensor, and find that the tensor representation of the ρ meson is more reliable in the description of the existing data. In particular, we show that the ρ-meson t-pole contribution, including the interference with an effective nonlocal contact term, sufficiently improves the description of the recent JLab data at invariant mass $W \lesssim 2.2$ GeV and $Q^2 \lesssim 2.5$ GeV$^2/c^2$. A "soft" variant of the strong πNN and ρNN form factors is also found to be compatible with these data. On the basis of the successful description of both the σ_L and σ_T parts of the cross section we discuss the importance of taking into account the σ_T data when extracting the charge pion form factor F_π from σ_L.

I. INTRODUCTION

The motivation of many experiments [1–6] on forward pion electroproduction at large Q^2 is the study (through measurements close to the pion mass shell) of the pion charge form factor $F_\pi(Q^2)$. For values of the s-channel $p + \gamma^*$ energy W above the resonance region and for small momentum-k ($k^2 = t$) transferred to the nucleon spectator the longitudinal part σ_L of the cross section is dominated by the t-channel quasielastic mechanism (see Fig. 1). In this case the πNN strong form factor $F_{\pi NN}^2(t) \approx 1$ is a slowly varying function at $|t| \approx M_\pi^2$ and

$$\sigma_L \sim \frac{|t| F_{\pi NN}^2(t)}{\left(t - M_\pi^2\right)^2} \sigma_{e\pi}^{\text{free}}, \qquad \sigma_{e\pi}^{\text{free}} \sim F_\pi^2(Q^2), \qquad (1)$$

where $\sigma_{e\pi}^{\text{free}}$ is the free $e\pi$ cross section. However, with currently available data [1–6] on the Rosenbluth separation of $\sigma = \sigma_L + \sigma_T$ the situation is not so simple. For comparison of data to theoretical predictions one should calculate both σ_L and σ_T parts of the cross section at least on the basis of a sum of the $s(u)$- and t-pole diagrams depicted in Fig. 2. It should be noted that the $s(u)$-channel contributions [Figs. 2(b) and 2(c)] to the forward pion cross section are suppressed [7] only at considerably high Q^2, i.e., in the region $Q^2 \gtrsim 2$–3 GeV$^2/c^2$, where the product of corresponding vertex form factors and propagators drop faster in Q^2 ($\sim Q^{-n}$, $n \gtrsim 4$) as compared to the $\sim Q^{-2}$ behavior of the pion form factor $F_\pi(Q^2)$. In this Q^2 region the forward pion cross section is not as large as for smaller $Q^2 \lesssim 1$ GeV$^2/c^2$ studied earlier [1,3], and until recently the available data on Rosenbluth separation were too poor [3,4] to be a reliable basis for the evaluation of $F_\pi(Q^2)$.

The high quality data recently obtained at JLab [5,6] for $Q^2 = 1.6$ and 2.45 GeV$^2/c^2$ can considerably aid in the study of $F_\pi(Q^2)$. However, at the values $W = 1.95$ and 2.2 GeV

characteristic of the high Q^2 JLab data (old and new) the kinematical limit for the momentum transfer $t_c \approx -(0.1$–$0.15)$ GeV$^2/c^2$ is not so close to the pion pole position as is the case for low $Q^2 \lesssim 1$ GeV$^2/c^2$. Thus the vertex dependence on t for all the diagrams in Fig. 2 becomes very important for the extraction of the pion form factor $F_\pi(Q^2)$ from the data on σ_L.

In this context the existing data on σ_L and σ_T available now [3,5,6] for a large region of momentum transfers $0.05 \lesssim -t \lesssim 0.5$ GeV$^2/c^2$ can also be used for the study of the strong meson-nucleon form factors $F_{\pi NN}(t)$, $G_{\rho NN}(t)$, and $F_{\rho NN}(t)$ in parallel to the study of $F_\pi(Q^2)$. The direct measurement of these form factors would be very useful for both meson-exchange models of the nuclear force [8] and of exchange currents in nuclei [9]. Cutoff parameters Λ_{MNN} ($M = \pi$ or ρ) used in the monopole parametrization

$$F_{\pi NN}(t) = \frac{F_{\pi NN}(0)}{1 - t/\Lambda_{\pi NN}^2}, \quad F_{\rho NN}(t) = \frac{F_{\rho NN}(0)}{1 - t/\Lambda_{\rho NN}^2} \quad (2)$$

are presently known only indirectly from data and values of Λ_{MNN} are varying in a wide interval of $M_\rho \lesssim \Lambda_{MNN} \lesssim 2M_\rho$ (exchange currents in nuclei are usually fitted with soft form factors with $\Lambda_{MNN} \approx M_\rho$, while the nucleon-nucleon interaction models require harder form factors with $\Lambda_{MNN} \approx 1.5$–2 M_ρ). On the other hand, in the constituent quark model (CQM) [10–12] the cutoff parameter Λ_{MNN}, at least for form factors at small values of $-t \lesssim 0.3$ GeV$^2/c^2$, is determined by the radius b of the three-quark system and for realistic values $b \approx 0.5$–0.6 fm one obtains $\Lambda_{MNN}^2 \approx 0.5$–0.7 GeV$^2/c^2$.

In Refs. [12,13] it was shown that the recent JLab data on forward pion electroproduction [3] are compatible with a soft πNN form factor. However, in Ref. [3] the data were described on the basis of a Regge model modified by introducing a common electromagnetic form factor $F_\pi(Q^2)$ for both t-channel and "Reggeized" s-channel amplitudes [14] as is schematically shown in Fig. 3. In this model proposed by Vanderhaeghen, Guidal, and Laget (VGL) there are no constraints on the maximum value of $|t|$ as the t-dependence

---

*On leave of absence from Department of Physics, Tomsk State University, RU-634050 Tomsk, Russia.
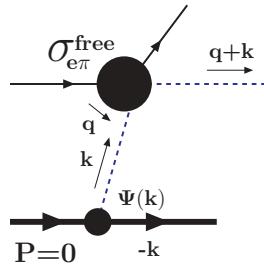
FIG. 1. (Color online) Dominating t-channel quasielastic mechanism for the longitudinal part σ_L of the cross section.

FIG. 3. (Color online) Factorization of the amplitude of pion electroproduction off the nucleon in the Regge model [14].

of the cross section is determined by the t-(and s-) behavior of the π- and ρ-Regge trajectories. The model of VGL offers a satisfactory explanation of both photo- and electroproduction data for pions in a large interval of t including the longitudinal part of the forward pion cross section σ_L measured at JLab, but fails in explaining the transverse part σ_T. The prediction for σ_T is about an order of magnitude smaller than measured values. At small $|t| \lesssim 0.3$ GeV$^2/c^2$ a conventional model predicts, on the basis of the t-pole contribution, the same results starting from the form factors (2) motivated by the CQM. This was shown in our previous work [13] by comparison of predictions for σ_L made in both models. The situation for σ_T is also similar (see below), i.e., at small t, an approach using strong vertex form factors based on the CQM is equally good in the explanation of σ_L, but also fails for σ_T.

In both models the ρ exchange has little influence on σ_L for small values of $-t$, while σ_T is rather sensitive to this contribution. Hence, a comprehensive analysis of the role of the ρ meson for describing the transverse cross section σ_T is required. Since the introduction and discovery of the vector meson resonances their special role was recognized in phenomena both in nuclear and particle physics [15]. Essential properties of vector mesons (e.g., the ρ meson) such as universality and dominance in electromagnetic hadronic form factors had a large impact on the understanding of the electromagnetic structure of hadrons. Since the early sixties attempts to include the vector mesons in the formalism of quantum field theory have been initiated (see [15] and references therein) including effective chiral Lagrangian approaches [16–26]. A detailed investigation of different ways to include massive vector mesons in the effective low-energy Lagrangians has been performed in Ref. [21]. In particular, it was shown that the pure tensor representation of vector mesons is most natural for constructing their coupling to pseudoscalar mesons

and photons (the extension onto the baryon sector was done in Ref. [22]) consistent with chiral symmetry, vector meson dominance (VMD), and asymptotic QCD behavior. However, the conventional vector representation of vector mesons is in conflict with VMD and the asymptotic properties of QCD [21]. In Ref. [21] for the example of the pion electromagnetic form factor, it was demonstrated in the context of chiral perturbation theory (ChPT) [19,27] how to remedy the shortcomings of the vector representation: an appropriate local term of order of $O(p^4)$ has to be introduced in addition. The corresponding coupling of the local term was fixed to achieve a complete agreement between the two schemes based on the tensor and vector field representations of the vector mesons.

Chiral symmetry plays an important role in the low-energy domain (below 1 GeV) of quantum chromodynamics: it governs the strong interaction between hadrons. All known low-energy approaches (effective field theories, different types of quark models, etc.) in the study of the properties of light hadrons have to incorporate the concept of at least an approximate chiral symmetry to get reasonable agreement with data. In our case, contrary to what might be naively expected for the high energy process $p(e.e'\pi)n$, the t-channel contribution [Fig. 2(a)] to the quasielastic pion knockout corresponds to a transfer of low energy $k_0 = t/2m_N$ and momentum $|\mathbf{k}| = \sqrt{k_0^2 - t}$ to the nucleon spectator, and thus a low-energy approach to the t-channel terms might well be substantiated.

However, in practice we have the interplay of two energy regimes: on the one hand the low-energy dynamics of nucleons with low-momentum π- and ρ-mesons in the t-channel, and on the other hand the initial photon with a large Euclidean momentum transfer squared $Q^2 \gtrsim 1$–2 GeV$^2/c^2$ and the final pion with a large energy $E_\pi \gtrsim 2$ GeV. The diagrams contributing to the pion electroproduction in the relevant kinematical regime are displayed in Fig. 2: t-channel resonance diagrams with π and ρ exchange in Fig. 2(a), s- and u-pole diagrams with the intermediate nucleon and a tower of nucleon resonances in
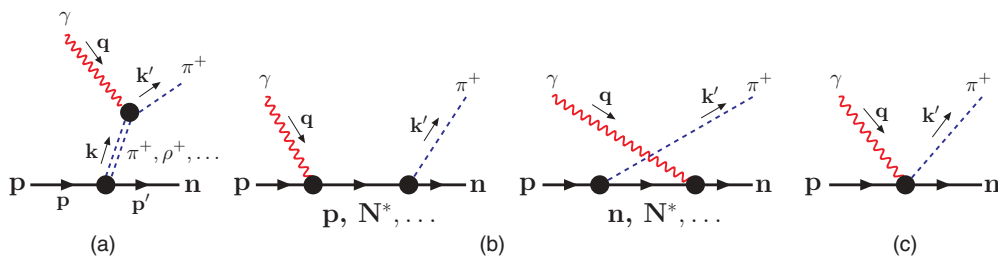

FIG. 2. (Color online) Feynman diagrams ("Born approximation") for the pion electroproduction off the nucleon.

Fig. 2(b) and the contact $\gamma \pi N N$ diagram (the Kroll-Ruderman term) of Fig. 2(c).

On the basis of these Feynman diagrams the main objective of the present work is to study how the predictions for σ_L and σ_T depend on the ρ meson representation. In our calculations we accept the following strategy.

First, we consider the transverse cross section σ_T and show that it can be well described by taking the ρ meson-exchange diagram only. The quality of the description is valid up to $Q^2 \simeq 2$ GeV^2. To our knowledge this is the first successful description of σ_T including the special role of the intermediate ρ meson. We test both representations of the ρ meson: tensor and vector. Our result is that the tensor representation gives a sufficiently better description of σ_T. Of course, both representations can be put in equivalence following the idea of Ref. [21] by adding an appropriative local term to the Lagrangian of the vector representation. We do not resort to this procedure, instead we argue that the pure tensor variant is more appropriate from a phenomenological point of view and constraints dictated by VMD and the asymptotic QCD behavior.

Second, we consider the longitudinal cross section σ_L and show that this quantity asks for a more sophisticated interplay of different diagrams from the set of Fig. 2. Any description of the $s(u)$-channel contributions to σ_L in terms of nucleon resonances would be rather complicated and might lead to doubtful results. Here we follow the results of our recent work [13]. On the basis of a quark model it was shown that in the region of intermediate Q^2 ($\gtrsim 1$–2 GeV^2/c^2) the effective description of $s(u)$-channel and contact-term contributions might be reduced to a renormalization of the Kroll-Ruderman contact term modified by strong and electromagnetic form factors. The renormalization constant is the sole free parameter which we fit to the σ_L data.

Our main finding is that a realistic description of both σ_L and σ_T can be obtained in a t-channel $\pi + \rho$ approach with standard values of coupling constants and cutoff parameters, if (i) we use the tensor representation for the ρ meson leading to the reproduction of data on the transverse cross section; (ii) we approximate the sum of all the s-channel diagrams in Figs. 2(b) and 2(c) by a single effective contact term of type Fig. 2(c) with a phenomenological form factor. For simplicity and to reduce the number of possible free parameters we choose the cutoff parameter in this form factor to be close to the one used, e.g., in the $\rho \pi \gamma$ form factor. The normalization of this term is fitted to the σ_L data.

In the present manuscript we proceed as follows. First, in Sec. II we discuss the basic notions of our approach. We derive the effective Lagrangian for the description of pion electroproduction off the nucleon. We discuss different field representations of the ρ meson. Then we discuss the contributions of different Born diagrams to the amplitude of pion electroproduction. In Sec. III we discuss the choice of hadronic form factors parametrizing finite size effects due to hadronic interactions including the photons. In Sec. IV our results are presented in comparison to the JLab data and to the predictions of the VGL model. Finally, in Sec. V we give a short summary of our results and discuss the importance

of taking into account the σ_T data when extracting F_π values from the data on σ_L.

II. EFFECTIVE LAGRANGIAN AND MATRIX ELEMENTS

Our considerations for the pion electroproduction are based on an effective Lagrangian approach. It involves nucleon, pion, ρ meson, and photon degrees of freedom. The finite size effects of hadronic interactions are parametrized by corresponding form factors.

A. Inclusion of nucleons, pions, and photons

The part of the full Lagrangian including the doublet of nucleons $N = (p, n)$, the triplet of pions $\vec{\pi}$ and the electromagnetic field A_μ is motivated by chiral perturbation theory (ChPT) [19,27,28] and has the standard form

$$\mathcal{L}_{\text{eff}} = \bar{N}(\not{D} - m_N)N + \frac{1}{2}\big[D_\mu \vec{\pi} D^\mu \vec{\pi} - M_\pi^2 \vec{\pi}^2\big]$$
$$- \frac{g_A}{2F_\pi}\bar{N} D_\mu \vec{\pi} \vec{\tau} \gamma^\mu \gamma^5 N - \frac{1}{4}F_{\mu\nu}F^{\mu\nu} + \cdots, \quad (3)$$

where $\pi^\pm = -(\pi_1 \mp i\pi_2)/\sqrt{2}$, $\pi^0 = \pi_3$, $F_{\mu\nu} = \partial_\mu A_\nu - \partial_\nu A_\mu$ is the stress tensor of the electromagnetic field, g_A is the nucleon axial charge, F_π is the leptonic decay constant, $m_N \equiv m_p = 938.27$ MeV and $M_\pi \equiv M_{\pi^\pm} = 139.57$ MeV are nucleon and pion masses. The symbol $\cdots$ denotes terms of higher order not needed in our consideration. In the numerical calculations we express $g_A/(2F_\pi) = g_{\pi NN}/(2m_N)$ through the strong $\pi N N$ coupling constant using the Goldberger-Treiman relation with $g_{\pi NN} = 13.5$. The covariant derivative D_μ, containing the electromagnetic field and acting on proton and charged pion fields, is defined as $D_\mu p = (\partial_\mu - ieA_\mu)p$ and $D_\mu \pi^\pm = (\partial_\mu \mp ieA_\mu)\pi^\pm$, where e is the proton charge. For neutral fields (neutron and π^0) D_μ coincides with ordinary derivative. The inclusion of the ρ meson and the addition of strong and electromagnetic form factors in the effective Lagrangian (3) will be discussed below. Note, in addition to the more convenient pseudovector (PV) coupling of the pion to nucleons [the third term in the right hand side of Eq. (3)] we also consider the pseudoscalar (PS) coupling: $\mathcal{L}_{\pi NN}^{PS} = g_{\pi NN}\bar{N} i\gamma^5 \vec{\pi} \vec{\tau} N$.

B. Inclusion of vector mesons

For the ρ meson we use two different field representation: tensor and vector. Here we follow Refs. [19–22,24]. In the tensor representation the triplet of ρ mesons is written in terms of antisymmetric tensor fields: $\rho_{\mu\nu}^W = -\rho_{\nu\mu}^W = (\vec{\rho}^W \vec{\tau})_{\mu\nu}/\sqrt{2}$. The free Lagrangian of vector mesons in the tensor representation is written in the form

$$\mathcal{L}_\rho^W = -\frac{1}{2}\partial^\mu \rho_{\mu\nu}^{Wa} \partial_\alpha \rho_a^{W\alpha\nu} + \frac{M_\rho^2}{4}\rho_{\mu\nu}^{Wa} \rho_a^{W\mu\nu}. \quad (4)$$

The ρ-meson propagator in the tensor representation has the form

$$
\begin{aligned}
G_{W;\mu\nu,\alpha\beta}^{ab}(x-y) &= \langle 0|T\{\rho_{\mu\nu}^{Wa}(x), \rho_{\alpha\beta}^{Wb}(y)\}|0\rangle \\
&= -\frac{\delta^{ab}}{M_\rho^2}\int\frac{d^4k}{(2\pi)^4 i}\frac{e^{ik\cdot(x-y)}}{M_\rho^2-k^2-i\epsilon} \\
&\quad \times\left[g_{\mu\alpha}g_{\nu\beta}(M_\rho^2-k^2)\right. \\
&\quad \left.+ g_{\mu\alpha}k_\nu k_\beta - g_{\mu\beta}k_\nu k_\alpha - (\mu\leftrightarrow\nu)\right],
\end{aligned}
\tag{5}
$$

where the terms in the square brackets proportional to $(M_\rho^2 - k^2)$ will generate contact terms in the vector-meson exchange interaction.

Now we turn to a discussion of the vector representation of ρ mesons, i.e., in terms of the vector fields ρ_μ. The corresponding free Lagrangian has the form

$$
\mathcal{L}_\rho^V = -\frac{1}{4}\rho_{\mu\nu}^{Va}\rho^{Va\mu\nu} + \frac{M_V^2}{2}\rho_\mu^a\rho^{a\mu},
\tag{6}
$$

where $\rho_{\mu\nu}^{Va} = \partial_\mu\rho_\nu^a - \partial_\nu\rho_\mu^a$. For the sake of comparison between the two different representation it is convenient to write down the propagator in the vector representation as a t-product of $\rho_{\mu\nu}^V$:

$$
\begin{aligned}
G_{V;\mu\nu,\alpha\beta}^{ab}(x-y) &= \langle 0|T\{\rho_{\mu\nu}^{Va}(x), \rho_{\alpha\beta}^{Vb}(y)\}|0\rangle \\
&= -\frac{\delta^{ab}}{M_V^2}\int\frac{d^4k}{(2\pi)^4 i}\frac{e^{ik\cdot(x-y)}}{M_V^2-k^2-i\epsilon} \\
&\quad \times[g_{\mu\alpha}k_\nu k_\beta - g_{\mu\beta}k_\nu k_\alpha - (\mu\leftrightarrow\nu)].
\end{aligned}
\tag{7}
$$

As was stressed in Ref. [21] the propagators $G_{W;\mu\nu,\alpha\beta}^{ab}$ and $G_{V;\mu\nu,\alpha\beta}^{ab}$ differ by the contact term contained in the tensorial propagator:

$$
\begin{aligned}
&G_{W;\mu\nu,\alpha\beta}^{ab}(x) \\
&= G_{V;\mu\nu,\alpha\beta}^{ab}(x) + \frac{i}{M_V^2}[g_{\mu\alpha}g_{\nu\beta} - g_{\mu\beta}g_{\nu\alpha}]\delta^{ab}\delta^4(x).
\end{aligned}
\tag{8}
$$

Therefore, the use of the two different representations leads to a different off-shell behavior of vector meson-exchange diagrams. As we already mentioned in the Introduction, a detailed analysis of vector and tensor schemes was performed in Ref. [21] for the example of the electromagnetic pion form factor. The tensor representation was found to be fully consistent with constraints of chiral symmetry, VMD and the asymptotic behavior of QCD. To get equivalence of the two representations a certain inclusion of an additional local term was required. In our analysis we find that the tensor representation for the vector mesons is more reliable and leads to an understanding of the transverse cross section of the pion electroproduction in the considered kinematical situation. In particular, the additional contact term in the propagator of the tensor representation considerably modifies the ρ-exchange contribution to the cross section.

According to [22,24], a chirally invariant Lagrangian for the couplings of the tensor field $\rho_{\mu\nu}^W$ to baryons can be written in the general form containing couplings which can be related to the ones of the commonly used vector representation. Therefore, we further proceed using the vector representation for the

ρNN couplings:

$$
\mathcal{L}_{\rho NN} = \frac{1}{2}\bar{N}\left(G_{\rho NN}\vec{\rho}_\mu\gamma^\mu - \frac{F_{\rho NN}}{2m_N}\sigma^{\mu\nu}\partial_\nu\vec{\rho}_\mu\right)\vec{\tau}N.
\tag{9}
$$

The anomalous $\rho\pi\gamma$ coupling is defined as

$$
\mathcal{L}_{\rho\pi\gamma}^{V(W)} = \frac{eM_\rho}{4}g_{\rho\pi\gamma}\varepsilon^{\mu\nu\alpha\beta}F_{\mu\nu}\vec{\rho}_{\alpha\beta}^{V(W)}\vec{\pi}.
\tag{10}
$$

The coupling constant $g_{\rho\pi\gamma} = 0.728$ GeV^{-1} is fixed from the $\rho\to\pi\gamma$ decay width:

$$
\Gamma(\rho\to\pi\gamma) = \frac{\alpha}{24}g_{\rho\pi\gamma}^2 M_\rho^3\left[1 - \frac{M_\pi^2}{M_\rho^2}\right]^3,
\tag{11}
$$

where $\alpha = 1/137.036$ is the fine-structure constant. In our convention the isospin symmetric hadron masses of the isomultiplets are identified with the masses of the charged partners:

$$
m_N = m_p = 938.27 \text{ MeV}, \quad M_\pi = M_{\pi^\pm} = 139.57 \text{ MeV},
\tag{12}
$$

$$
M_\rho = M_{\rho^\pm} = 775.5 \text{ MeV}.
$$

C. Born diagrams contributing to the pion electroproduction

In the calculation of the amplitude for the pion electroproduction off the nucleon we restrict to the Born approximation. At the order of accuracy we are working in we include t-channel diagrams with ρ and π exchange [Fig. 2(a)], s- and u-channel diagrams with intermediate nucleons [Fig. 2(b)] and in the case of the pseudovector coupling of pions to nucleons we have the extra diagram [Fig. 2(c)], the so-called Kroll-Ruderman term, describing the contact coupling of the photon to two nucleons and one pion.

1. Contribution of the ρ-meson exchange diagram

We start with the discussion of the ρ-meson exchange diagram. Despite the difference between the propagators and between the $\rho\pi\gamma$ couplings in the respective representations the final expression has a common universal form. For the ρ-meson exchange diagram contribution to the pion electroproduction amplitude [Fig. 2(a)] for both the W and V variants we have

$$
\begin{aligned}
T_\rho^{\begin{Bmatrix} V \\ W \end{Bmatrix}}(\lambda, s, s') &= \frac{e}{2\sqrt{2}}g_{\rho\pi\gamma}\varepsilon_{\mu\nu}^{(\lambda)}(q)\bar{u}_n(p', s') \\
&\times\Bigg\{\left[G_{\rho NN} + \frac{\begin{Bmatrix} k^2 \\ M_\rho^2 \end{Bmatrix}}{4m_N^2}F_{\rho NN}\right]\frac{2m_N}{M_\rho^2-k^2}\sigma^{\mu\nu}\gamma_5 \\
&\quad -\frac{2m_N}{M_\rho^2-k^2}\bigg[G_{\rho NN}\frac{P^\mu\gamma^\nu - P^\nu\gamma^\mu}{2m_N} \\
&\quad -F_{\rho NN}\frac{P^\mu k^\nu - P^\nu k^\mu}{4m_N^2}\bigg]i\gamma_5\Bigg\}u_p(p, s),
\end{aligned}
\tag{13}
$$

where $P = p + p', k = p - p'$ and s, s' denote the spin projections of the initial proton and final neutron, respectively;

$\varepsilon_{\mu\nu}^{(\lambda)}(q) = q_\mu \epsilon_\nu^{(\lambda)}(q) - q_\nu \epsilon_\mu^{(\lambda)}(q)$. Here $\epsilon_\mu^{(\lambda)}(q)$, with $\lambda = 0, \pm 1$, are basis vectors of circular polarization for the virtual photon quantized along the momentum **q**, i.e., they are defined as

$$\epsilon^{(\lambda=0)\mu}(q) = \left\{ \frac{|\mathbf{q}|}{Q}, 0, 0, \frac{q_0}{Q} \right\},$$

$$\epsilon^{(\lambda=\pm 1)\mu}(q) = \left\{ 0, \mp\frac{1}{\sqrt{2}}, \frac{-i}{\sqrt{2}}, 0 \right\}, \quad Q = \sqrt{-q^2}. \tag{14}$$

The vectors $\epsilon_\mu^{(\lambda)}(q)$ satisfy the conventional orthogonality, normalization and completeness conditions [29]

$$q^\mu \epsilon_\mu^{(\lambda)}(q) = 0, \quad \epsilon^{(\lambda)\mu}(q)\epsilon_\mu^{(\lambda')*}(q) = (-1)^\lambda \delta^{\lambda\lambda'},$$

$$\sum_{\lambda=0,\pm 1} (-1)^\lambda \epsilon_\mu^{(\lambda)}(q)\epsilon_\nu^{(\lambda)*}(q) = g_{\mu\nu} - \frac{q_\mu q_\nu}{q^2}. \tag{15}$$

In Eq. (13) the factor $\{ {}^{k^2}_{M_\rho^2} \}$ in the first square brackets should be taken equal to k^2 for the vector V-variant and equal to M_ρ^2 for the tensor W-variant. From Eq. (13) one can conclude that the results for the W and V variants are degenerate when $k^2 \to M_\rho^2$, but in the region $(M_\rho^2 - k^2) \approx m_N^2$ characteristic of the JLab data [3–6] they are considerably different. The corresponding ρ-induced $\gamma\pi NN$ "contact" interaction arising in the tensor variant can be defined as

$$T_\rho^W - T_\rho^V = \frac{e}{4m_N\sqrt{2}} g_{\rho\pi\gamma} F_{\rho NN} \epsilon_{\mu\nu}^{(\lambda)}(q)$$

$$\times \bar{u}_n(p', s')\sigma^{\mu\nu}\gamma_5 u_p(p, s). \tag{16}$$

It should be noted that the difference encoded in the pion electroproduction amplitude in the contact term (16) is sufficient to get a good description of the transverse cross section σ_T.

2. Contribution of the π-meson exchange diagram

The pion t-pole diagram [Fig. 2(a)] gives the following contribution to the amplitude:

$$T_\pi(\lambda, s, s') = e\sqrt{2} g_{\pi NN} \frac{\epsilon^{(\lambda)}(q) \cdot (k + k')}{M_\pi^2 - k^2}$$

$$\times \bar{u}_n(p', s')i\gamma_5 u_p(p, s), \tag{17}$$

where $k = p - p'$, $t = k^2$, $k' = k + q$, $k'^2 = M_\pi^2$, and $q^2 = -Q^2$.

3. Nucleon s- and u-pole diagrams

The sum of the nucleon s- and u-pole diagram contributions to the total amplitude is

$$T_{N(s+u)}(\lambda, s, s')$$

$$= -e\sqrt{2} g_{\pi NN} \epsilon_\mu^{(\lambda)}(q)\bar{u}(p', s')\left[\left\{ \begin{array}{c} i\gamma_5 \\ \frac{i k\!\!\!/\gamma_5}{2m_N} \end{array} \right\} \frac{p\!\!\!/ + q\!\!\!/ + m_N}{W^2 - m_N^2} \right.$$

$$\times \left(F_{1p}\gamma^\mu + F_{2p}\frac{i\sigma^{\mu\nu}q_\nu}{2m_N} \right) - \left(F_{1n}\gamma^\mu + F_{2n}\frac{i\sigma^{\mu\nu}q_\nu}{2m_N} \right)$$

$$\times \frac{p\!\!\!/ - k\!\!\!/' + m_N}{W^2 + Q^2 + t - M_\pi^2 - m_N^2}\left\{ \begin{array}{c} i\gamma_5 \\ \frac{i k\!\!\!/\gamma_5}{2m_N} \end{array} \right\}\right] u(p, s), \tag{18}$$

where $s = (p + q)^2 = W^2$ and $u = (q - p')^2 = -W^2 - Q^2 - t + 2m_N^2 + M_\pi^2$. Here the factors $i\gamma_5$ or $\frac{k\!\!\!/\gamma_5}{2m_N}$ in the column $\{\cdots\}$ correspond to the pseudoscalar (PS) or pseudovector (PV) πNN coupling, respectively. The coupling constants F_{iN} equal

$$F_{1p} = 1, \quad F_{1n} = 0, \quad F_{2p} = \mu_p - 1, \quad F_{2n} = \mu_n, \tag{19}$$

where μ_p and μ_n are magnetic moments of proton and neutron.

4. The $\gamma\pi NN$ contact diagram

The $\gamma\pi NN$ contact diagram of Fig. 2(c) only shows up for the case of the PV variant. The corresponding amplitude is (we denote it by the subscript "CPV," that is contact pseudovector coupling):

$$T_{\text{CPV}}(\lambda, s, s') = -\frac{e\sqrt{2} g_{\pi NN}}{2m_N}\bar{u}(p', s') \epsilon\!\!\!/^{(\lambda)}(q)i\gamma_5 u(p, s). \tag{20}$$

Finally, we make a comment concerning the interference of the ρ-exchange amplitude with other contributions in the calculation of the cross section. In the vector variant the interference term between the T_π- and T_ρ^V-pole diagrams does not contribute to the σ_L and σ_T cross sections. However, in the tensor variant the interference term between the T_π- and T_ρ^W-pole diagrams is not negligible (see below) and thus we should consider the interference terms for all the potentially important diagrams including the $s(u)$-channel diagrams [Fig. 2(b)].

III. FORM FACTORS

A. General consideration

Up to now we deal with diagrams generated by the effective Lagrangian involving nucleons, pions, the ρ meson, and the photon (see discussion in previous section). It can be easily checked that the sum of Born diagrams (Fig. 2) is gauge invariant. For example, the hadronic electromagnetic current $\langle p's'|J_{\text{Born}}^\mu|ps\rangle$ defined as

$$\epsilon_\mu^{(\lambda)}\langle p's'|J_{\text{Born}}^\mu|ps\rangle = T_\rho(\lambda, s, s') + T_\pi(\lambda, s, s')$$

$$+ T_{n(s+u)}(\lambda, s, s') + T_{CPV}(\lambda, s, s') \tag{21}$$

satisfies current conservation $q_\mu\langle p's'|J_{\text{Born}}^\mu|ps\rangle = 0$. Note, that the ρ-meson exchange and pion-pole diagrams satisfy current conservation separately, while $s(u)$-pole and contact Kroll-Ruderman term are separately do not satisfy this condition (i.e., only in sum).

Now we are in the position to modify the vertices describing strong and electromagnetic interactions of hadrons—by introducing hadronic form factors. The idea of such a modification is clear: we would like to include finite size effects. The introduction of form factors into the interaction Lagrangian and, therefore, into the Born amplitudes leads to a violation of gauge invariance. To restore gauge invariance one can use different methods (see, e.g., discussion in Refs. [30–35]). One of the methods is based on the Gross-Riska procedure [30], which does the following modification in matrix elements: every term containing form factor F which is multiplied with

γ-matrix and vector P^μ with open Lorentz index μ coinciding with the index of the photon polarization vector is modified as [30]

$$\gamma^\mu F \rightarrow \gamma^\mu F + q^\mu \frac{\slashed{q}}{q^2}(1 - F) = \gamma_\perp^\mu F + q^\mu \frac{\slashed{q}}{q^2},$$

$$P^\mu F \rightarrow P^\mu F + q^\mu \frac{Pq}{q^2}(1 - F) = P_\perp^\mu F + q^\mu \frac{Pq}{q^2}, \quad (22)$$

where $\gamma_\perp^\mu = \gamma^\mu - q^\mu \slashed{q}/q^2$ and $P_\perp^\mu = P^\mu - q^\mu Pq/q^2$ are the Dirac matrix and momentum which are orthogonal to photon momentum and are obtained from original quantities by multiplying with the projector $g_{\mu\nu}^\perp = g_{\mu\nu} - q_\mu q_\nu/q^2$. Note that the idea suggested in [30] was extended to pion electroproduction in [32] and was extensively used in Refs. [33,34]. In particular, the Gross-Riska procedure leads to the correct low-energy theorems and guarantees that the partial conservation of axial current (PCAC) constraint for the pion electroproduction amplitude is satisfied [33].

In this paper we use the similar method of restoring electromagnetic gauge invariance which is fully equivalent to the Gross-Riska prescription [30] when we fulfill the additional conditions (16), i.e., use the circular polarization for the virtual photon field. In particular, our modification of matrix elements reads as

$$\gamma^\mu F \rightarrow \gamma_\perp^\mu F,$$

$$P^\mu F \rightarrow P_\perp^\mu F. \quad (23)$$

An advantage of our method is that each diagram is separately satisfy the current conservation by construction, due to $q_\mu \gamma_\perp^\mu = 0$ and $q_\mu P_\perp^\mu$. It is sufficient in our consideration while instead of sum of the $s(u)$-pole and local Kroll-Ruderman term we will use the modified Kroll-Ruderman term with form factor (see discussion below), which should satisfy the current conservation separately.

When introducing form factors, in the fit to data we intend to deal with a minimal amount of free parameters which should be common for both variants of the ρ representation. For this purpose we use a common form factor of a simple monopole form (2) for all the strong meson-nucleon vertices with the same cutoff parameter Λ_{str}:

$$g_{\pi NN} \rightarrow g_{\pi NN}(t) = g_{\pi NN} F_{str}(t),$$

$$G_{\rho NN} \rightarrow G_{\rho NN}(t) = G_{\rho NN} F_{str}(t),$$

$$F_{\rho NN} \rightarrow F_{\rho NN}(t) = F_{\rho NN} F_{str}(t), \quad (24)$$

$$F_{str}(t) = \frac{1}{1 - t/\Lambda_{str}^2}.$$

We vary the parameter Λ_{str}^2 in the region 0.5–0.7 GeV^2/c^2 (which is close to the CQM predictions) to fit the JLab data on σ_L.

The form factors for the electromagnetic vertices are known with better accuracy, both for the pion and the nucleon. We use a monopole parametrization for the pion

$$e \rightarrow e F_\pi(Q^2), \quad F_\pi(Q^2) = \frac{1}{1 + Q^2/\Lambda_\pi^2}, \quad (25)$$

where Λ_π^2 should be close to its mean value of $\Lambda_\pi^2 \approx 0.54$ GeV^2/c^2, and the dipole parametrization for the electromagnetic Sachs form factors of nucleons.

The form factor of the $\rho\pi\gamma$ vertex is the most uncertain since at this vertex two variables, t and Q^2, are off-shell (for the $\pi\pi\gamma$ vertex, where the situation is similar, we neglect the t dependence, since for the forward pion electroproduction t, as a rule, is close to its on-mass shell value of $t = M_\pi^2$). For reasons motivated by the CQM we modify the $\rho\pi\gamma$ vertex as

$$g_{\rho\pi\gamma} \rightarrow g_{\rho\pi\gamma}(t, Q^2) = g_{\rho\pi\gamma} F_{\rho\pi\gamma}(t, Q^2), \quad (26)$$

where for the form factor $F_{\rho\pi\gamma}(t, Q^2)$ we take the combined expression

$$F_{\rho\pi\gamma}(t, Q^2) = \frac{1}{1 + (M_\rho^2 - t)/(4M_\rho^2)} \frac{1}{1 + Q^2/\Lambda_{eff}^2}. \quad (27)$$

We consider only two possibilities for the Q^2 behavior:

(a) $\Lambda_{eff} = \Lambda_\pi$, the "soft" variant,

(b) $\Lambda_{eff} \gtrsim 2\Lambda_\pi$, the "hard" variant.

In the "hard" variant Λ_{eff} is considered as a free parameter close to the usual values of $\Lambda_\rho \approx 1$–1.2 GeV/c [5,14]. We will fit Λ_{eff} to the JLab data on σ_T.

In conclusion we shortly formulate/repeat a common rule for all the vertices where a pion is created or annihilated. In the Born expression for such a vertex

(i) $e F_\pi(Q^2)$ should be substituted for the charge e,

(ii) $g_{\pi NN}(t)$ should be substituted for $g_{\pi NN}$.

This rule is extended to the contact term (20) as well (see below). The modification of the s- and u-channel contributions including the contact (Kroll-Ruderman) term will be discussed in the next subsection.

Some remarks on the t-dependence of Eq. (27) should be added. We use a "hard" cutoff parameter $2M_\rho$ for the t-dependence of the $\rho\pi\gamma$ vertex in both the time-like $t > 0$ and space-like $t < 0$ regions. In the space-like region the strong hadron form factors have been evaluated in many works (see, e.g., [8,9]) on the basis of a rich data base on NN scattering and exchange currents in nuclei, in which case the value of the cutoff parameter varies between M_ρ and $2M_\rho$. But our task is to evaluate the form factor in the time-like region on the basis of the σ_T data. Our efforts to describe σ_T with the soft cutoff parameter $\sim M_\rho$ fail since in this case the effective value of the $\rho\pi\gamma$ coupling in the region near $t \sim 0$ is suppressed by the factor $[1 + (M_\rho^2 - t)/M_\rho^2]^{-1} \sim 1/2$. This probably indicates that in the time-like region the cutoff parameter should be hard, and thus here we use the large value $2M_\rho$. We further do not vary this parameter to simplify handling other free parameters when fitting the cross section.

B. An effective description of s- and u-channel contributions

The only exclusion from rules (i) and (ii) is the πNN vertex in the nucleon s- and u-pole diagrams [Fig. 2(b)], where the pion is on its mass shell ($k'^2 = M_\pi^2$), but the intermediate nucleon, after absorption of a large $Q^2 \gtrsim m_N^2$ is severely off its mass shell. For this vertex we formally introduce a form factor
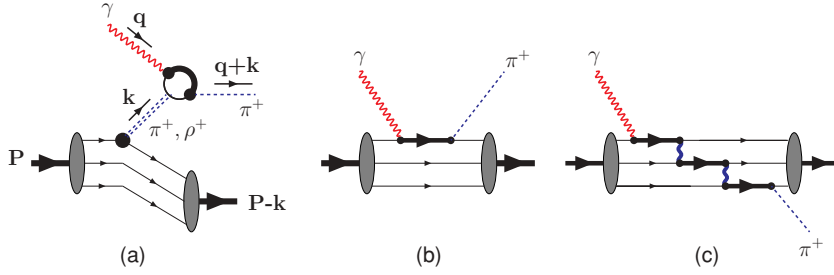
FIG. 4. (Color online) Microscopic interpretation of t- and s-channel processes within the quark model. Thick lines indicate the propagation of a large photon momentum q through separate partons inside the nucleon.

$F_{\text{eff}}(t, Q^2)$, but do not really use it in calculations since such a form factor should include contributions of all the excited baryon states compatible with a large virtual mass W in the s-channel.

Since a description in terms of baryon poles would be very complicated and in practice is beyond reach we turn from the hadron picture of the s-channel process to the quark model consideration following our recent work [13]. Such a consideration gives at least qualitative insight into the relevant processes when a large Q^2, induced by electroproduction of pions, is propagating through the three-quark system (Fig. 4). In the quark models three mechanisms are implied. The first one [Fig. 4(a)] corresponds to the t-channel hadron mechanism considered above with a small momentum transfer to the nucleon spectator. The other two mechanisms [Figs. 4(b) and 4(c)] generate amplitudes which differ in the power n of the large Q^2 behavior ($\sim Q^{-n}$). For the diagram of Fig. 4(c) the amplitude has an asymptotic behavior with $n \gtrsim 4$, while for the other one [Fig. 4(b)] n should be smaller and similar to the one of the pion form factor with $n = 2$.

Starting from this observation we discussed the above quark mechanisms in Ref. [13] in terms of a naive $^3P_0$ model [10,11] on the basis of a harmonic oscillator quark model. Our evaluation had shown that in this approximation the corresponding effective amplitude T_{eff} becomes proportional to the contact term (20) times the product of two form factors, the electric pion and strong πNN, i.e., $T_{\text{eff}} \sim T_{CPV} F_\pi(Q^2) F_{\pi NN}(t)$ (see Ref. [13] for detail). The resulting amplitude is perfectly in line with the above formulated empirical rules (i) and (ii).

However, at large Q^2 the $^3P_0$ model cannot be reliable in predictions for the Q^2 behavior of the amplitudes and thus, instead of the pion form factor $F_\pi(Q^2)$, we use the more general phenomenological form factor of the form

$$F_{\text{eff}}(Q^2) = \frac{1}{1 + Q^2/\Lambda_{\text{eff}}^2}. \tag{28}$$

For simplicity we use the same cutoff parameter Λ_{eff} for all the effective Q^2-dependent terms [see, for example, the analogous effective $\rho\pi\gamma$ form factor of Eq. (27)] .

From the above discussion follows that the effective description of $s(u)$-channel and contact-term contributions to the pion electroproduction amplitude at intermediate values of Q^2 might be reduced to a renormalization of the contact term modified by electric F_{eff} and strong F_{str} form factors

$$\{T_{N(s+u)} + T_{CPV}\}_{\text{eff}} \approx Z F_{\text{eff}}(Q^2) F_{\text{str}}(t) T_{CPV}. \tag{29}$$

In a simplified model here we consider this possibility by fitting the free parameter Z to the data on σ_L. Hence, the total amplitude is written in the form

$$T = T_\pi + T_\rho + Z F_{\text{eff}}(Q^2) F_{\text{str}}(t) T_{CPV}, \tag{30}$$

where T_{CPV} is the Born amplitude (20), while T_ρ and T_π are the amplitudes (13) and (17) modified by strong and electromagnetic form factors, respectively.

IV. RESULTS

In this section we discuss result of our calculation of the transverse and longitudinal cross sections.

The differential cross section for the $p(e, e'\pi^+)n$ reaction integrated over the azimuthal angle $\phi_{e'}$ of the electron in the one-photon approximation is usually defined [37] as

$$\int_0^{2\pi} \frac{d^5\sigma}{dE_{e'}d\Omega_{e'}d\Omega_{\pi'}^*}d\phi_{e'} = 2|\mathbf{q}^*||\mathbf{k}'^*|2\pi\Gamma_t\left\{\varepsilon\frac{d\sigma_L}{dtd\phi_{\pi'}^*}\right.$$
$$+\frac{d\sigma_T}{dtd\phi_{\pi'}^*} + \varepsilon\frac{d\sigma_{TT}}{dtd\phi_{\pi'}^*}$$
$$\left.+\sqrt{2\varepsilon(1+\varepsilon)}\frac{d\sigma_{LT}}{dtd\phi_{\pi'}^*}\right\}, \tag{31}$$

where ε is the invariant parameter used for the Rosenbluth separation of cross sections

$$\varepsilon = \left[1 + \frac{2\mathbf{q}^2}{Q^2}\tan^2\frac{\theta_{e'}}{2}\right]^{-1} = \left[1 + \frac{2\mathbf{q}^{*2}}{Q^2}\tan^2\frac{\theta_{e'}^*}{2}\right]^{-1} \tag{32}$$

and Γ_t is the "virtual-photon flux factor". In Eq. (31) and below the variables defined in the center-of-mass reference frame are denoted by an asterisk "*" while in the laboratory frame they are used without an asterisk, e.g.,

$$|\mathbf{q}| = \sqrt{\left(\frac{W^2 - m_N^2 + Q^2}{2m_N}\right)^2 + Q^2}, \quad |\mathbf{q}^*| = \frac{m_N}{W}|\mathbf{q}|,$$
$$\tag{33}$$
$$|\mathbf{q}_r^*| = |\mathbf{q}^*|_{Q^2=0} = \frac{W^2 - m_N^2}{2W}.$$

The final expressions for the longitudinal and transverse cross sections in the approximation of the lowest order t-, s-,

and u-channel diagrams (35) read

$$
\frac{d\sigma_L}{dt} = \mathcal{N}_\sigma \frac{1}{4\pi} \overline{|T(\lambda = 0)|^2},
$$

$$
\frac{d\sigma_T}{dt} = \mathcal{N}_\sigma \frac{1}{2} \sum_{\lambda = \pm 1} \frac{1}{4\pi} \overline{|T(\lambda)|^2},
$$

$$
\frac{d\sigma_{TT}}{dt} = \mathcal{N}_\sigma \left\{ -\frac{1}{2} \sum_{\lambda = \pm 1} \frac{1}{4\pi} \overline{T(\lambda)T(-\lambda)^*} \right\},
$$

$$
\frac{d\sigma_{LT}}{dt} = \mathcal{N}_\sigma \left\{ -\frac{1}{2} \sum_{\lambda = \pm 1} \lambda \left(\frac{\overline{T(0)T(\lambda)^*} + \overline{T(\lambda)T(0)^*}}{4\pi\sqrt{2}} \right) \right\},
$$

(34)

where $T(\lambda)$ is the pion electroproduction amplitude, which describe the π-, ρ-, nucleon-poles- and contact-term contributions to the hadron current

$$
\langle p', s' | \epsilon_\mu^{(\lambda)} J^\mu | p, s \rangle \equiv T(\lambda, s, s') = T_\pi(\lambda, s, s')
$$
$$
+ T_\rho^{\mathrm{W(v)}}(\lambda, s, s') + T_{N(s+u)}(\lambda, s, s')
$$
$$
+ T_{\mathrm{CPV}}(\lambda, s, s'). \quad (35)
$$

The common kinematical factor $\mathcal{N}_\sigma / 4\pi$ is defined by the standard expression

$$
\mathcal{N}_\sigma = \frac{1}{\sqrt{\left(W^2 - m_N^2 + Q^2\right)^2 + 4m_N^2 Q^2}} \frac{1}{W^2 - m_N^2}. \quad (36)
$$

The sum over spin projections

$$
\overline{|T(\lambda)|^2} = \frac{1}{2} \sum_{s,s'} |T(\lambda, s, s')|^2 \quad (37)
$$

in Eq. (34) can be calculated by the standard trace technique, and the calculation results in an universal formula for all the cross sections listed in Eq. (34). In the extended version of this paper which is available [38] we list the full analytical results for both longitudinal σ_L and transverse σ_T parts given for all the diagonal and interference terms.

For the results we have tested two approximations to the $s(u)$-channel amplitudes:

(i) the naive or "exact" representation (35) which makes use of the proper Feynman amplitudes (18) and (20) with an intermediate virtual nucleon;

(ii) the effective representation (30) [with two variants, "soft" (a) and "hard" (b), discussed in Sec. III below Eq. (27)] taking into account intermediate hadron states through quark diagrams giving the main contribution to the "s-channel part" of the cross section at large Q^2.

Here we furthermore use both the tensor (W) and vector (V) representation of the ρ-exchange amplitude.

Our calculation shows that approximation (i) is extremely unrealistic. The interference terms between the t-pole amplitudes and the "exact" $T_{N(s+u)} + T_{\mathrm{CPV}}$ amplitudes are too large. The resulting longitudinal cross section is in rather poor agreement with the observed data on σ_L. Only the diagonal terms without the $s(u)$-pole contributions give qualitative agreement with the σ_L data.

The approximation (ii) is more realistic. Results of this approximation are displayed in Figs. 5 and 6. By varying

the free parameter Z one can obtain a good description of both cross sections σ_L and σ_T for the tensor variant of the ρ-exchange amplitude (W). For the vector variant (V) only σ_L can be described in agreement with experimental data. However, the "soft" variant (a) with $\Lambda_{\mathrm{eff}} \approx \Lambda_\pi$ used in the form factors $F_{\rho\pi\gamma}(t, Q^2)$ and $F_{\mathrm{eff}}(Q^2)$ is less suitable for describing the existing data in a large interval of Q^2 from 0.6 to 2.45 GeV^2/c^2, since it fails to describe the slow Q^2 dependence of σ_T in the full interval. The experimental ratio $\sigma_T(Q^2 = 0.6)/\sigma_T(Q^2 = 2.45)$ is about 6, while the corresponding ratio of form factors squared $F_{\rho\pi\gamma}^2(Q^2 = 0.6)/F_{\rho\pi\gamma}^2(Q^2 = 2.45)$ multiplied by the kinematical factor $\mathcal{N}_\sigma$ Eq. (36) is several times larger.

Only the "hard" variant (b) with $\Lambda_{\mathrm{eff}} \gtrsim 2\Lambda_\pi$ is suitable in describing the data. Taking the value $\Lambda_{\mathrm{eff}} = 1.2$ GeV/c, which is close to the conventional values $\Lambda_\rho \approx 1$–1.2 used in literature for the $\rho\pi\gamma$ form factor (see, e.g., [5]), and taking the standard "soft" value $\Lambda_{\mathrm{str}}^2 = 0.7$ GeV^2/c^2 for the common strong form factor (25) we obtain a satisfactory description of both σ_L and σ_T cross sections in a wide interval of Q^2.

The values of the $\rho N N$ coupling constants were fixed to $G_{\rho NN}(0) = 4$ and $F_{\rho NN}(0) = 26$ close to the recommended in the ChPT approach [24] of $G_{\rho NN}(0) = 4$ and $F_{\rho NN}(0)/G_{\rho NN}(0) = 6.1$ (since the value of σ_T directly depends on $F_{\rho NN}$ we slightly corrected the conventional value of $F_{\rho NN}(0)$ to obtain the best description of the recent data [5] on σ_T for $Q^2 = 1.6$ GeV^2/c^2). In our calculation we only have one free parameter Z introduced in Eq. (30) as a phenomenological constant, which formally corresponds to a renormalization of the Born contact term T_{CPV} in the full amplitude (30); in essence the term $Z F_{\mathrm{eff}}(Q^2) F_{\mathrm{str}}(t) T_{\mathrm{CPV}}$ amounts to a phenomenological description of the s-channel contributions, which otherwise cannot be calculated from first principles. Based on general considerations (see Sec. III) we can only expect that such contributions are suppressed at large Q^2, and thus a small value of the phenomenological constant Z would be expected.

By varying Z one can improve the description of only one of the cross section component (on account of the another), σ_L or σ_T. To compare our results to the VGL model predictions [14], which are only realistic for σ_L, we fit the value of Z to the σ_L data in the full interval $0.6 < Q^2 < 2.45$ GeV^2/c^2. With a value of $Z = 0.11$ we obtain a description of σ_L which practically coincides (see Figs. 5 and 6) with the results of the recent Regge-model motivated description of the data [5,6].

The small value of Z correlates well with the quark mechanism proposed in Sec. III B for a description of s-channel contributions [Figs. 4(b) and 4(c)] to the cross section. In accordance with this picture, only a part of all the possible quark diagrams [Fig. 4(b)] survives at large Q^2, while the most part of diagrams [of the Fig. 4(c) type] is suppressed because of a high degree n of $\sim Q^{-n}$ behavior (it can be assumed that the value of Z corresponds to the weight $\sim 1/3$ of the surviving part of quark diagrams). On the other hand, it would be very difficult to describe this situation at large Q^2 starting from the interference of many baryon-resonance diagrams depicted in Fig. 2(b). Therefore, the smallness of Z can be considered as an argument in favor of the quark-model motivated representation of the transition amplitude
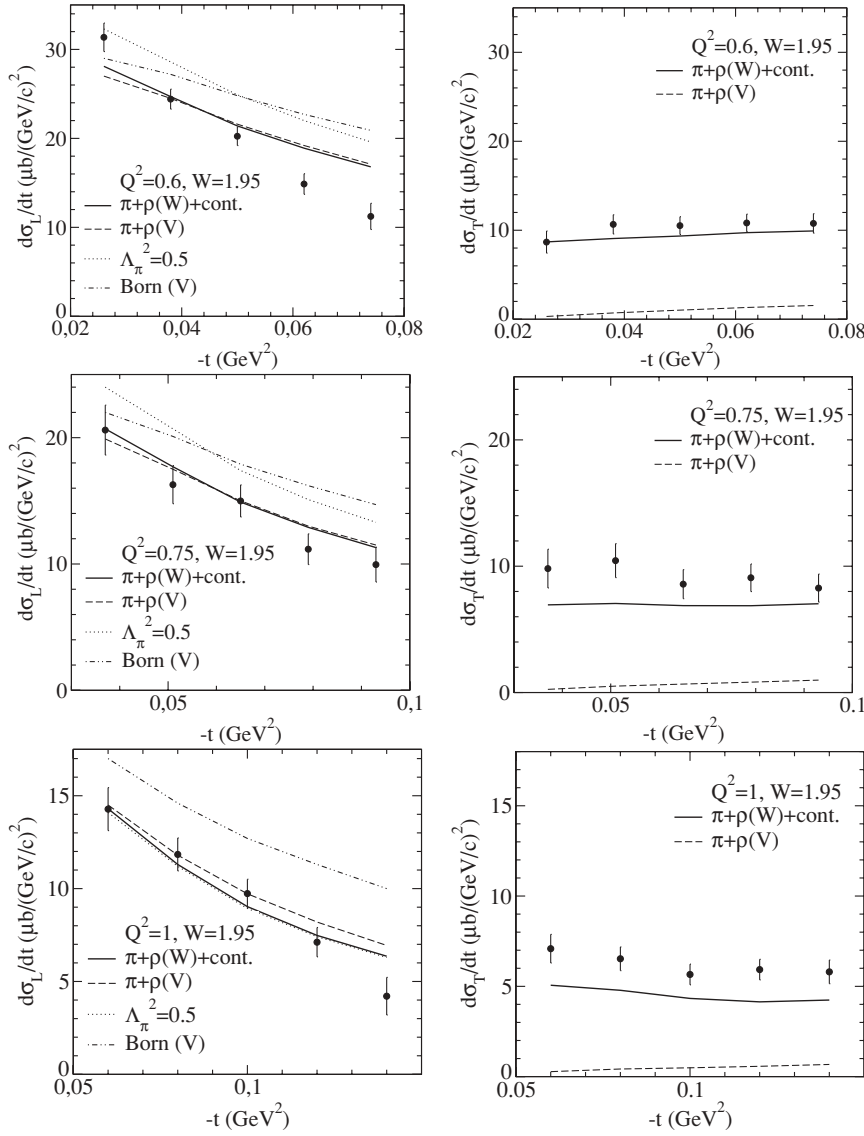
FIG. 5. Longitudinal and transverse cross sections for the $p(e, e'\pi^+)n$ reaction at small $Q^2 \lesssim 1$ GeV^2. The unscaled $F\pi 1$ data are centered at Q^2 of 0.6, 0.75, and 1 GeV^2. Interference terms between π-pole, ρ-pole, and contact $\pi\gamma NN$ amplitudes are taken into account. Results obtained in the t-pole approximation with the standard vector (V) ρ-meson field are shown by dashed lines. Results for the tensor variant (W) of the ρ-meson field (the contact diagram is included) are shown by solid lines (by dotted lines for the fixed value of $\Lambda_\pi^2 = 0.5$ GeV$^2/c^2$). Note that the proper values of W and Q^2 for each $-t$ bin are different and they differ from the average values shown in the figure legends (see [5,6] for detail). For comparison the proper Born approximation results (i.e., without the strong vertex form factors) are shown by double-dot dashed lines.

in Eq. (30) and against the naive hadron representation in Eq. (35).

Following Refs. [5,6], we use different values for the cutoff parameters Λ_π in the F_π form factor for sets of data centered at different values of Q^2. In Table I we compare the values of F_π (and correspondingly Λ_π) obtained by such a method to the values F_π obtained in Refs. [5,6] on the basis of the VGL model. The coupling constants and cutoff parameters used in the calculation are listed in Table II.

In the case of the vector variant V, which (as is also the case for the VGL model) describes only σ_L and fails for σ_T, the extracted values of F_π are close to the results of Refs. [5,6].

TABLE I. Comparison of results for the pion form factor $F_\pi(Q^2)$.

	Fπ1 data [6]				Fπ2 data [5]	
Q^2(GeV$^2/c^2$)	0.6	0.75	1	1.6	1.6	2.45
F_π [5,6]	0.433 ± 0.017	0.341 ± 0.022	0.312 ± 0.016	0.233 ± 0.014	0.243 ± 0.012	0.167 ± 0.010
$F_\pi(V)$	0.412	0.348	0.309	0.239	0.242	0.168
$\Lambda_\pi^2(V)$	0.420	0.400	0.447	0.503	0.511	0.494
$F_\pi(W)$	0.420	0.368	0.335	0.294	0.272	0.200
$\Lambda_\pi^2(W)$	0.434	0.437	0.504	0.666	0.597	0.614

TABLE II. Coupling constants and cutoff parameters.

$g_{\pi NN}$	$g_{\rho\pi\gamma}$ GeV^{-1}	$G_{\rho NN}(0)$	$F_{\rho NN}(0)$	Z	Λ^2_{str} GeV^2/c^2	Λ^2_{eff} GeV^2/c^2
13.5	0.728	4	26	0.11	0.7	1.44

For the tensor variant W our values for F_π differ from the ones of Refs. [5,6], but in this case we obtain a satisfactory description of σ_T as a byproduct of our approach.

It is evident that the proper form factor F_π cannot fluctuate sharply in magnitude from one Q^2 to another and the same is true for Λ_π used for its parametrization. However, after smoothing out the fluctuations one can see that there are two Q^2 regions, $Q^2 \lesssim 1$ GeV^2/c^2 and $Q^2 \gtrsim 1$ GeV^2/c^2, with different mean values for Λ_π. For our W variant we take $\Lambda^2_\pi = 0.5$ GeV^2/c^2 in the region of smaller $Q^2 \leqslant 1$ GeV^2/c^2 and $\Lambda^2_\pi = 0.6$ GeV^2/c^2 in the Q^2 region of the recent JLab experiment (in this case in the full interval the mean value of

TABLE III. Predicted values of Λ^2_π for a variety of theoretical approaches.

Λ^2_π (GeV^2/c^2)	Theory
0.51	Extended Nambu-Jona-Lasinio model [35]
0.52	Bethe-Salpeter/Schwinger-Dyson equations [40]
0.54	Light front dynamics [41]
0.55	Relativistic quark model [36]
0.60	Nonlocal chiral quark model [42]
0.66	Bethe-Salpeter/Schwinger-Dyson equations [43]
0.66	QCD sum rules [44]

Λ^2_π is about 0.54 GeV^2/c^2) and recalculate the cross section σ_L (in practice σ_T does not depend on small F_π variations). The dotted lines in Figs. 5 and 6 show how $\sigma_L(W)$ behaves for these averaged values of F_π. For comparison, the predicted values of Λ^2_π for a variety of theoretical approaches are shown in Table III.
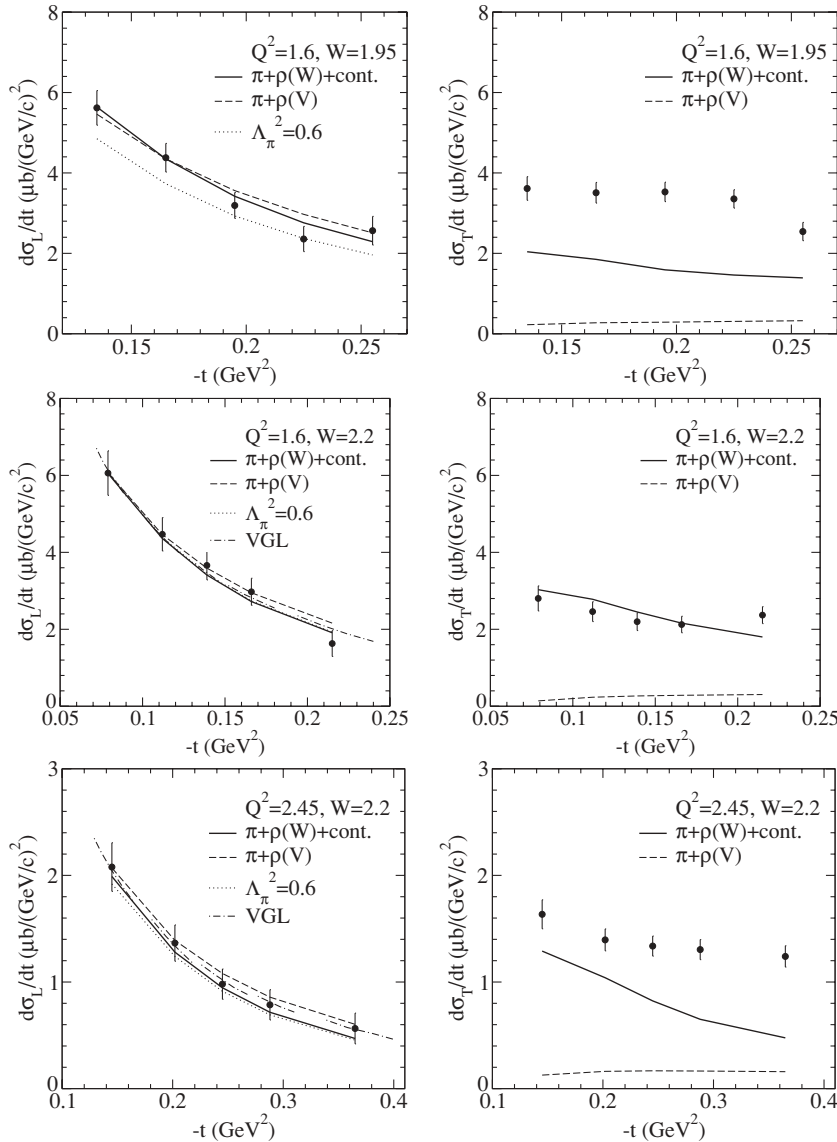

FIG. 6. Longitudinal and transverse cross sections at larger values of Q^2: 1.6 GeV^2/c^2 for the $F\pi1$ data and 1.6 and 2.45 GeV^2/c^2 for the $F\pi2$ data. The same notation as in Fig. 5. The dotted lines correspond to the fixed value of $\Lambda^2_\pi = 0.6$ GeV^2/c^2. Here for comparison the VGL model results (adapted from Ref. [5]) are shown by dash-dotted lines.

V. SUMMARY AND CONCLUSIONS

We analyzed pion electroproduction $p(e, e'\pi^+)n$, which was intensively studied at JLab in the quasielastic regime [3–6] for the original purpose of directly measuring the pion charge form factor $F_\pi(Q^2)$. Our framework is based on an effective Lagrangian approach involving nucleon, pion, ρ meson, and photon degrees of freedom. In the description of the ρ meson we test two possibilities: the so-called vector (V) and tensor (W) variants. For the standard vector variant V the transverse part σ_T of the cross section is considerably underestimated, whether it is the Regge model motivated approach VGL [14] or the traditional Born one [39] modified by strong form factors and contact terms [12,13]. Here we have shown that the problem of underestimating σ_T might be solved by taking into account specific contact terms in the ρ meson propagator that can be most naturally obtained in terms of the tensor variant W of the ρ meson description [20,24].

Based on these findings the uniqueness of the F_π data extracted from the σ_L cross section appears doubtful without taking into account the associated data on σ_T. The modified Born approach presented here is successful in the description of both the σ_L and σ_T cross sections, thus present a new possibility for the discussion of this problem.

First it should be noted that our results obtained for the standard variant V (the dashed lines in Figs. 5 and 6 for $d\sigma_L/dt$) obviously contradict the claim that the Born (i.e., the Feynman tree diagrams) approach is completely unsuited for the description of the forward pion electroproduction process. In our opinion a refined version of this statement would be more adequate: the Born approach is only unsuited for the photoproduction ($Q^2 = 0$) and for the low Q^2 region of electroproduction, but at intermediate and high Q^2 this approach becomes suitable. This statement is substantiated by a series of previous works [12,13,45,46] and in particular, by the present detailed evaluation. It seems likely that with growing Q^2 the full sum (not the isolated terms) of $s(u)$-channel contributions is decreasing most and while the t-pole contributions remain. However, any description of such Q^2 behavior in terms of many baryon poles would be rather complicated and, as a result, very doubtful. We can only use physical arguments based on the comparison of $d\sigma_L/dt$ data to the respective t-pole contributions depicted in Figs. 5 and 6 for variant V (the dashed line). One can see that starting at $Q^2 = 0.75 \, \text{GeV}^2/c^2$ the t behavior of the measured $d\sigma_L/dt$ is in good agreement with predictions given by the t-pole contributions

(but the agreement breaks down for $Q^2 = 0.6 \, \text{GeV}^2/c^2$ and for smaller Q^2 as our evaluation shows).

Second, the present successful description of σ_T on the basis of the tensor variant W raises another issue that finally remains to be resolved. Namely, for the variant V, which is very similar in results to the VGL model predictions, there is no π-ρ interference contribution to σ_L since the corresponding spin average term vanishes (see Appendices in the extended version [38]). But in the more realistic variant W this term does not vanish and cannot be neglected. In other words, in a realistic variant of the description of both σ_L and σ_T the ρ-exchange term influences not only σ_T but σ_L as well. Hence, the procedure of extracting F_π values from the σ_L data alone can, in principle, not be independent from a parallel description of the σ_T data. We evaluated such a possible indirect influence of the σ_T data on the final F_π values extracted from the recent JLab data (see last two rows in Table I). In our simplified model for the W variant, including a phenomenological contact term (proportional to the free parameter Z), we obtained values for F_π which differ from previous ones (extracted without taking into account the σ_T data) by about 10–15% at $Q^2 \gtrsim 1.6 \, \text{GeV}^2/c^2$. This deviation is traced to the ρ-π interference, which cannot be neglected. It counts rather in favor of the value $\Lambda_\pi^2 \approx 0.6 \, \text{GeV}^2/c^2$ obtained in our approach than in favor of the value $\Lambda_\pi^2 \approx 0.5 \, \text{GeV}^2/c^2$ obtained on the basis of the VGL model. However, now we cannot obtain trustworthy values for the uncertainties $\pm\Delta\Lambda_\pi^2$ because of the considerable model dependence of the s-channel contributions to σ_L.

In the future we intend to extend our formalism to the study of kaon electroproduction in connection with the recent JLab experiment E93-018 [47].

[1] P. Brauel *et al.*, Z. Phys. C **3**, 101 (1979).

[2] C. J. Bebek *et al.*, Phys. Rev. D **17**, 1693 (1978).

[3] J. Volmer *et al.* (The Jefferson Lab F(pi) Collaboration), Phys. Rev. Lett. **86**, 1713 (2001); J. Volmer, Ph.D. thesis, Vrije Universiteit, Amsterdam, 2000 (unpublished).

[4] G. Huber, D. Mack, and H. Block, JLab experiment E01-004(2003); E. J. Beise, AIP Conf. Proc. **698**, 23 (2004); Nucl. Phys. **A751**, 167 (2005).

[5] T. Horn *et al.* (Fpi2 Collaboration), Phys. Rev. Lett. **97**, 192001 (2006).

[6] V. Tadevosyan *et al.* (Jefferson Lab F(pi) Collaboration), Phys. Rev. C **75**, 055205 (2007).

[7] J. Speth and V. R. Zoller, Phys. Lett. **B351**, 533 (1995); N. N. Nikolaev, A. Szczurek, and V. R. Zoller, Z. Phys. A **349**, 59 (1994).

[8] R. Machleidt, K. Holinde, and C. Elster, Phys. Rep. **149**, 1 (1987).

[9] D. O. Riska, Phys. Rep. **181**, 207 (1989).

[10] A. Le Yaouanc, L. Oliver, O. Pene, and J. C. Raynal, Phys. Rev. D **8**, 2223 (1973).

[11] E. S. Ackleh, T. Barnes, and E. S. Swanson, Phys. Rev. D **54**, 6811 (1996); S. Capstick and W. Roberts, *ibid*. **49**, 4570 (1994); C. Downum, T. Barnes, J. R. Stone, and E. S. Swanson, Phys. Lett. **B638**, 455 (2006).

[12] V. G. Neudatchin, I. T. Obukhovsky, L. L. Sviridova, and N. P. Yudin, Nucl. Phys. **A739**, 124 (2004).

[13] I. T. Obukhovsky, D. Fedorov, A. Faessler, T. Gutsche, and V. E. Lyubovitskij, Phys. Lett. **B634**, 220 (2006).

[14] M. Vanderhaeghen, M. Guidal, and J. M. Laget, Phys. Rev. C **57**, 1454 (1998); M. Guidal, J. M. Laget, and M. Vanderhaeghen, Nucl. Phys. **A627**, 645 (1997).

[15] J. J. Sakurai, *Currents and Mesons*, Chicago Lectures in Physics (The University of Chicago Press, Chicago and London/ New York, 1969).

[16] J. S. Schwinger, Phys. Lett. **B24**, 473 (1967); J. Wess and B. Zumino, Phys. Rev. **163**, 1727 (1967); S. Weinberg, *ibid*. **166**, 1568 (1968).

[17] U. G. Meissner, Phys. Rep. **161**, 213 (1988).

[18] M. Bando, T. Kugo, and K. Yamawaki, Phys. Rep. **164**, 217 (1988).

[19] J. Gasser and H. Leutwyler, Ann. Phys. (NY) **158**, 142 (1984).

[20] G. Ecker, J. Gasser, A. Pich, and E. de Rafael, Nucl. Phys. **B321**, 311 (1989).

[21] G. Ecker, J. Gasser, H. Leutwyler, A. Pich, and E. de Rafael, Phys. Lett. **B223**, 425 (1989).

[22] B. Borasoy and U. G. Meissner, Int. J. Mod. Phys. A **11**, 5183 (1996).

[23] M. C. Birse, Z. Phys. A **355**, 231 (1996).

[24] B. Kubis and U. G. Meissner, Nucl. Phys. **A679**, 698 (2001).

[25] T. Fuchs, M. R. Schindler, J. Gegelia, and S. Scherer, Phys. Lett. **B575**, 11 (2003).

[26] M. R. Schindler, J. Gegelia, and S. Scherer, Eur. Phys. J. A **26**, 1 (2005).

[27] S. Weinberg, Physica A **96**, 327 (1979).

[28] J. Gasser, M. E. Sainio, and A. Svarc, Nucl. Phys. **B307**, 779 (1988).

[29] V. M. Budnev, I. F. Ginzburg, G. V. Meledin, and V. G. Serbo, Phys. Rep. **15**, 181 (1975).

[30] F. Gross and D. O. Riska, Phys. Rev. C **36**, 1928 (1987).

[31] K. Ohta, Phys. Rev. C **40**, 1335 (1989); H. Ito, W. W. Buck, and F. Gross, *ibid*. **43**, 2483 (1991); M. A. Ivanov, M. P. Locher, and V. E. Lyubovitskij, Few-Body Syst. **21**, 131 (1996).

[32] S. Nozawa, B. Blankleider, and T. S. H. Lee, Nucl. Phys. **A513**, 459 (1990); S. Nozawa and T. S. H. Lee, *ibid*. **A513**, 511 (1990).

[33] S. Scherer and J. H. Koch, Nucl. Phys. **A534**, 461 (1991).

[34] J. W. Bos, S. Scherer, and J. H. Koch, Nucl. Phys. **A547**, 488 (1992).

[35] I. V. Anikin, M. A. Ivanov, N. B. Kulimanova, and V. E. Lyubovitskij, Z. Phys. C **65**, 681 (1995).

[36] A. Faessler, T. Gutsche, M. A. Ivanov, V. E. Lyubovitskij, and P. Wang, Phys. Rev. D **68**, 014011 (2003).

[37] E. Amaldi, S. Fubini, and G. Furlan, *Pion Electroproduction* (Springer, Berlin, 1979); D. Drechsel and M. M. Giannini, Rep. Prog. Phys. **52**, 1083 (1989).

[38] A. Faessler, T. Gutsche, V. E. Lyubovitskij, and I. T. Obukhovsky, arXiv:0706.1844 [hep-ph].

[39] F. Gutbrod and G. Kramer, Nucl. Phys. **B49**, 461 (1972); A. Actor, J. G. Korner, and I. Bender, Nuovo Cimento A **24**, 369 (1974).

[40] P. Maris and P. C. Tandy, Phys. Rev. C **62**, 055204 (2000).

[41] F. Cardarelli, I. L. Grach, I. M. Narodetskii, E. Pace, G. Salme, and S. Simula, Phys. Rev. D **53**, 6682 (1996).

[42] A. E. Dorokhov, A. E. Radzhabov, and M. K. Volkov, Eur. Phys. J. A **21**, 155 (2004).

[43] C. D. Roberts, Nucl. Phys. **A605**, 475 (1996).

[44] V. A. Nesterenko and A. V. Radyushkin, Phys. Lett. **B115**, 410 (1982); JETP Lett. **39**, 707 (1984) [Pisma Zh. Eksp. Teor. Fiz. **39**, 576 (1984)].

[45] N. P. Yudin, L. L. Sviridova, and V. G. Neudachin, Phys. Atom. Nucl. **61**, 1577 (1998) [Yad. Fiz. **61**, 1689 (1998)].

[46] V. G. Neudachin, L. L. Sviridova, and N. P. Yudin, Phys. Atom. Nucl. **64**, 1600 (2001) [Yad. Fiz. **64**, 1680 (2001)].

[47] R. M. Mohring *et al.* (E93018 Collaboration), Phys. Rev. C **67**, 055205 (2003).